Inter-membrane adhesion mediated by mobile linkers: Effect of receptor shortage†

Susanne Franziska Fenz,‡*[a] Ana-Sunčana Smith,[bc] Rudolf Merkel[a] and Kheya Sengupta[d]

Received 17th June 2010, Accepted 4th October 2010
DOI: 10.1039/c0sm00550a

Giant unilamellar vesicles (GUVs) adhering to supported bilayers were used as a model system to mimic ligand–receptor mediated cell-cell adhesion. We present the effect of varying the concentration of receptors (neutravidin on the bilayer) and ligands (biotin on the vesicle) on GUV adhesion and the organization of receptors in the adhesion zone. At high concentrations of both ligands and receptors, the adhesion is strong, all the available membrane is adhered and receptors are accumulated under the adhered membrane up to the geometrical limit of close packing. At low concentrations of receptors (<0.5%), and an arbitrary concentration of ligands (≥0.1%), adhesion does not proceed to completion: the membrane is only partially bound and parts of it still fluctuate. The receptors tend to accumulate under the adhered membrane but the filling is partial. Receptors get jammed and form clusters with fractal like shapes along the rim of the adhered vesicle in such a way that the annular cluster prevents further filling of the adhesion disc. We characterize the filling in terms of a compaction factor and the final concentration. Interestingly, the closing of the ring of jammed clusters switches the interior of the adhesion disc from one thermodynamic ensemble to another. In the new ensemble the receptors sealed within the adhesion disc are mobile but their number is fixed. Under such conditions, the usually strong neutravidin/biotin bond is weak. The incomplete adhesion state can be attributed to a combination of the effects of diffusion, jamming and the competition of enthalpy and entropy on bond formation. The formation of jammed receptor clusters reported here represents a new mechanism that influences membrane adhesion.

1 Introduction

Inter-cellular adhesion is essential for the existence of multicellular organisms, providing not only mechanical linkage between cells but also mediating inter-cellular communication. Cell-cell adhesion is achieved *via* highly specific proteins that reside either in or on the cell membrane and are mobile in the plane of the membrane at least during a part of their lifetime. Active formation of inter-cellular contacts and the resulting redistribution of cell surface molecules are important steps in several vital processes including embryogenesis and wound healing. While our knowledge of the biochemistry of adhesion, including the intracellular signalling cascades that regulate it, is vast and ever expanding, a lot still needs to be understood about biophysical aspects of adhesion of cell membranes. One of the reasons for this is the difficulty of interpreting the physical response of a complex and out-of-equilibrium object like a living cell in a systematic and quantitative manner. One increasingly popular strategy to circumvent this issue is the use of cell mimetic model systems.[1–8] Here we adopt this strategy to explore inter-cellular membrane adhesion using a giant unilamellar vesicle (GUV) to mimic one cell membrane and a supported lipid bilayer to mimic the other cell membrane.

Membrane adhesion, in general, is mediated by a combination of generic physical forces and specific ligand–receptor interactions. In vesicles, adhesion leads to shape changes with corresponding membrane bending which costs energy. In addition, there is an energy loss due to a change in excess membrane area arising from the shape change associated with adhesion.[9] This last term leads to an augmentation in tension due to adhesion. In the absence of specific interactions the equilibrium shape of the vesicle is determined by a balance of adhesion, bending and tension.

Whenever specific ligand–receptor pairs, rather than generic physical forces, mediate the adhesion, the entropy of the ligands and the receptors also contribute to the effective adhesion energy.[10] In case of inter-membrane adhesion, usually both the ligands and the receptors are initially mobile. After bond formation, the number of independently moving particles is reduced, leading to a considerable loss in translational entropy. As a result the thermodynamic system reaches its state of minimal free energy by trading translational entropy for binding enthalpy. Thus, the number of formed bonds depends on the affinity of the ligand–receptor pairs.

Interestingly, it is now increasingly recognized that the affinity of the ligand–receptor pairs measured in solution, which can be

[a]*Institute of Bio- and Nanosystems 4: Biomechanics, Research Centre Jülich, 52425 Jülich, Germany. E-mail: fenz@physics.leidenuniv.nl*
[b]*Institute of Theoretical Physics II, University of Stuttgart, 70550 Stuttgart, Germany*
[c]*Institute of Theoretical Physics and Excellence Cluster, Engineering of advanced materials, University Erlangen-Nürnberg, 91052 Erlangen, Germany*
[d]*CNRS UPR 3118, Centre Interdisciplinaire de Nanosciences de Marseille, Aix-Marseille Université Campus de Luminy, 13288 Marseille cedex 9, France*

† Electronic supplementary information (ESI) available: Overview figure of representative vesicles for cases I, II, V and VI. See DOI: 10.1039/c0sm00550a

‡ Current address: Leiden Institute of Physics, Leiden University, 2333 CA Leiden, The Netherlands. E-mail: fenz@physics.leidenuniv.nl

thought of as the "intrinsic affinity" can be different from the effective affinity of the same pair while embedded in two dimensional soft membranes. While early ideas mainly focused on the re-binding probability[11] and force probe stiffness,[12] more recent work has explored the role of fluctuations and predicts a dependence of the affinity on ligand–receptor concentration.[13,14]

In inter-membrane adhesion, mobile ligands and receptors diffuse into the adhesion zone between the adhering membranes. If the gain in binding enthalpy exceeds the loss in translational entropy, bonds form and the bound molecules accumulate in the contact zone. Recent experimental and theoretical work has demonstrated that receptor accumulation is present also in model GUV/SLB systems and arises as a consequence of the passive thermodynamic response of such a system.[2,4,15] Indeed, for living cells, one of the earliest events in cell adhesion is the accumulation of receptors in the cell-cell contact zone. This had been already shown in early studies on cells adhering to bio-functionalized lipid vesicles.[16,17] It was further shown that such accumulation is associated with an increase in adhesion strength. In a series of pioneering studies, the group of Dustin[11,18] explored the role of the dissociation constant in this accumulation.

It is increasingly well recognized that the surface of a living cell is very crowded, resulting in strong interactions of steric and other origin that lead to a drastic depression in diffusivity of membrane proteins.[19,20] The adhesion induced accumulation discussed above can be expected to make the environment even more crowded. Indeed, in an earlier work we showed that in a model GUV/SLB system, increasing accumulation not only immobilized the binding proteins but also slowed down the diffusion of membrane lipids because they encountered obstacles that were slower or even immobile.[2]

From the above discussion a strong link can be expected between adhesion, re-scaling of bonding affinity, receptor accumulation and receptor diffusion, but such a chain of effects has hitherto not been probed either in cells or in model systems. In this article we address this issue and show, for the first time, that scarcity of receptors gives rise to characteristic receptor accumulation patterns.

Our model system consists of giant vesicles (GUVs), whose membrane, containing ligands (biotinylated lipids), interacts with supported bilayers (SLBs) containing receptors (biotinylated lipids, which are further decorated with fluorescent neutravidin, an avidin analogue). We probed membrane adhesion with interference microscopy and receptor accumulation with fluorescence microscopy. At high receptor concentration, tight inter-membrane adhesion was achieved, whereas at low receptor concentrations, the membrane did not fully bind. This is consistent with expectations from simple thermodynamic arguments, if the effective binding energy is in fact lower than the intrinsic binding energy reported in literature. We performed competitive unbinding experiments that showed that indeed the bonds are weaker than expected. Complementary fluorescence microscopy showed that receptors accumulated into the partially bound adhesion zone. Characteristic ring-like patterns of jammed accumulated receptors with fine, fractal-like structures were seen. Their specific form can be explained on the basis of scaling arguments on receptor diffusion and accumulation. The jamming of receptors reported here even at low receptor concentrations represents a new mechanism that influences membrane adhesion.

2 Data analysis

Multi-interface RICM and construction of height maps

The adhered vesicles were probed with reflection interference contrast microscopy (RICM, see ref. 21 for a recent review). The recorded image, which is in the form of a matrix of intensities $I(h)$, is converted to a matrix or map of corresponding heights h of the vesicle membrane above the substrate. In brief, first a precise theoretical relation between $I(h)$ and the corresponding h was obtained, taking into account reflections from five interfaces as required for a GUV/SLB system.[22,23] To facilitate later numerical calculations, this intensity as a function of height was appropriately normalized and fitted with:

$$I_{\mathrm{norm}}(h) = y_0 - A\cos\left(\frac{4\pi n_{\mathrm{out}}}{\lambda}(h - h_0)\right) \quad (1)$$

where y_0, A and h_0 are free parameters, $n_{\mathrm{out}} = 1.3350$ is the refractive index of the buffer and $\lambda = 546$ nm is the wavelength of light. Measured intensities were normalized with respect to the measured background intensity and were converted to heights by inverting eqn (1), using the previously fitted parameters. It should be noted that in contrast to traditional RICM analysis on the basis of two reflections only, lower intensities do no longer necessarily correspond to lower heights. For details see ref. 22, 23.

Dynamical RICM and construction of fluctuation maps

Dynamical reflection interference contrast microscopy (Dy-RICM)[15] quantifies thermal fluctuations of soft interfaces. In this technique, the suppression of fluctuations is used as a signature of adhesion. To quantify fluctuations, first, the membrane topographies were constructed from 30 consecutive RICM images in a time sequence by application of eqn (1). Next, a pixel-by-pixel map of the fluctuation amplitude, defined as the standard deviation of the height over the entire sequence, was constructed. Since the apparent height fluctuations h_{fluc} could arise either from a real change in the height of the membrane or from recorded intensity fluctuations originating from the intensity dependent camera shot noise h_{shot},[23] the fluctuation map was normalized with respect to h_{shot}[24] to obtain $\phi = h_{\mathrm{fluc}}/h_{\mathrm{shot}}$. Due to the limited number of frames analyzed, the value of ϕ in the background, where only pure camera noise was expected, was slightly higher than the theoretically expected value of one. Based on measurements in the background, $\phi \geq 1.5$ was taken to represent real fluctuations of the GUV's membrane, whereas smaller values were interpreted as pure shot noise.

Construction of fluorescence maps

Fluorescence images were corrected for inhomogeneous illumination by fitting a two dimensional parabola to the background, and subtracting the resulting surface from the original image. Finally, fluorescence maps were constructed where each pixel was displayed in a color-coded fashion in units of background fluorescence. Here background fluorescence was set by the

specifics of sample preparation and was defined as the intensity measured outside the vesicle adhesion area. The concentration of fluorescent receptors in the adhesion area could be determined from comparison of the measured intensities within and outside of the adhesion area.[2]

Quantification of receptor accumulation

The accumulation of the fluorescent receptors was quantified in terms of the final maximum concentration of receptors in the contact zone c_f^{max}. Since the intensity is directly proportional to the concentration, $c_f^{max} = A^{max}\, c_i$ where c_i is the initial receptor concentration on the SLB and A^{max} is the maximum normalized intensity observed. c_f^{max} is thus the absolute maximum concentration reached in the contact zone in %. The index "max" refers to the fact that the maximum rather than the average concentration in the adhesion zone is reported to account for the inhomogeneous cases.

Determination of the compaction factor or filling efficiency

Patterns formed by accumulated fluorescent receptors were analyzed using a box counting procedure. The fluorescence images were first segmented to generate masks for the accumulated areas, choosing an appropriate threshold for each case, calculated with respect to the background in such a way that accumulated and non-accumulated areas were clearly separated. A grid consisting of squares with edge length l was overlaid on the masks and the number of squares necessary to cover the accumulation pattern was counted. Length, l, was successively lowered and the procedure repeated till the whole pattern was covered. The number of squares $N(l)$ needed to cover the pattern is given by a power law $N(l) = Bl^{-\alpha}$ where B is a constant and α is the filling factor. The $\ln(N)$ was plotted against l, and α was determined by fitting a straight line to the data in the linear regime. This procedure is equivalent to finding the fractal dimension of an object. We present normalized values of the filling factor $\alpha_{norm} = \frac{\alpha}{\alpha_{HR}}$ where α_{HR} is the measured non-normalized filling factor at high receptor density. Thus, complete filling observed at maximum receptor packing yielded the value unity.

All analysis, including RICM, Dy-RICM, fluorescence and box counting, was done using self-written routines in Matlab (R2008a, The MathWorks, Natick, MA).[25]

3 Results and discussions

Binding of the membrane observed by RICM

The functionalized giant unilamellar vesicles (GUV) were sedimented on functionalized supported lipid bilayers (SLB). Initially, the GUVs hovered over the SLBs at a distance of about 90 nm forming a quasi-flat, well defined contact zone with strong membrane fluctuations. At this stage, the interaction potential is given mainly by a balance of unspecific interactions: gravity, van der Waals attraction and Helfrich repulsion, which add up to form a shallow energy minimum at a distance of about 90 nm from the substrate. This results in very weak adhesion. The initial spheroidal shape of the vesicle was deformed to a truncated spheroid and the global shape was determined by a balance of effective adhesion energy, elastic deformation and tension. We define the *contact zone* as comprising of those parts of the membrane that are closer than a threshold distance of h_1 from the substrate (here $h_1 = 135$ nm, corresponding to the first bright fringe in the RICM micrograph). This definition is useful since this part of the membrane was available for specific adhesion without changing the global shape of the vesicle and thus costing very little elastic energy to enter the specifically adhered state.

Eventually, ligand–receptor bonds started to form in the contact zone, thus establishing a specific adhesion zone. We define the *adhesion zone* as the area where the fluctuations of the vesicle membrane are suppressed to the level of the camera shot noise. In this specifically adhered state the membrane substrate distance ranges from about 5 nm to up to 15 nm.

Depending on receptor and ligand concentrations, the dwelling time before the observation of bond clusters ranged from a few minutes to approximately 30 min. Whether or not specific adhesion proceeded to completion, or, in other words, whether the entire contact zone became an adhesion zone or only parts of it, depended on the concentration of ligands and receptors present in the system. Six different combinations of receptor and ligand concentrations were studied (see Table 1 for an overview). Fig. 1 shows the RICM images together with the calculated height and fluctuation maps for the two limiting cases of high (case I) and low (case VI) receptor–ligand concentration (see Fig. S1, in the ESI† for other combinations of concentrations).

If the concentration of receptors on the SLB was high (cases I, II and III), adhesion was complete and thermal fluctuations of the membrane within the whole contact zone were totally suppressed (see Table 2 and Fig. 1 I c). In other words, the adhesion zone occupied 100% of the contact zone. Neither the edges of the contact zone nor trapped bubbles or blisters inside the contact zone exhibited any fluctuations. We concluded that all the available receptors were bound resulting in high effective adhesion energy densities. That, in turn, ensured that the vesicles adhered and spread until all the excess area available prior to adhesion was used up and the increasing membrane tension suppressed all fluctuations. It can be expected that the new shape is determined by the balance of the effective adhesion energy–arising mainly due to bond formation,[10] with elastic deformation and adhesion induced tension.[9,26]

At low receptor concentrations (cases IV, V and VI) vesicles adhered only partially and the adhesion zone occupied only about 90% of the contact zone (see Fig. 1 II c). The vesicles,

Table 1 The different combinations of ligands (given as concentration of biotinylated lipids in the GUVs) and receptors (given as concentration of biotinylated lipids in the SLBs—this was directly equal to the number of neutravidin binding sites available on the SLBs) studied herein. Each combination is assigned a number for easy identification in the text

	SLB			
GUV	1%	0.5%	0.25%	0.1%
1%			IV	V
0.5%	I	III		
0.1%	II			VI

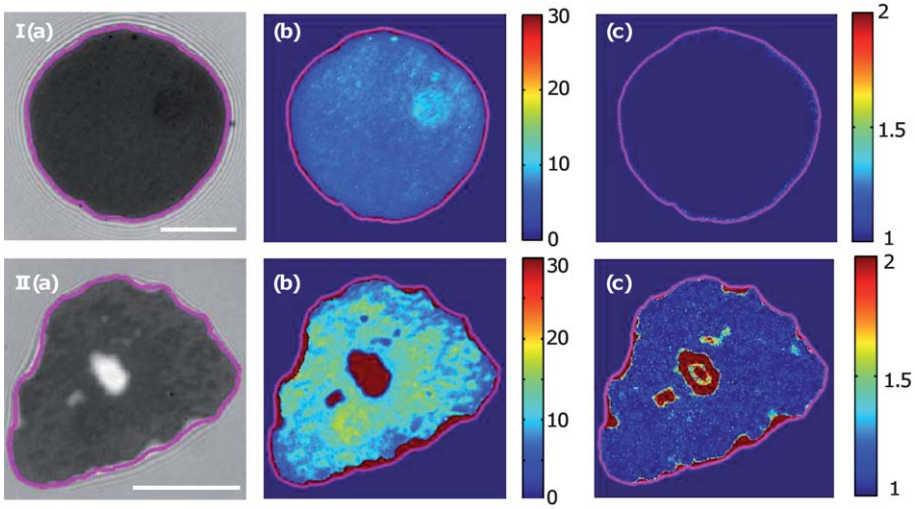

Fig. 1 Representative vesicles in the final adhesion state from the two limiting cases. I: Case I (1% SLB, 0.5% GUV), II: Case VI (0.1% SLB, 0.1% GUV). (a) RICM image averaged over 30 frames. The pink line encloses the contact zone. (b) Height map (nm). (c) Normalized fluctuation map (no unit). Scale bar: 10 μm.

Table 2 Table showing a summary of the obtained results for each case identified in Table 1. R_{adh}: The ratio of the area of the adhesion zone and the area of the final contact zone expressed as a mean percentage [%] ± the standard deviation of their distribution. c_f^{max}: Maximum receptor concentration in the adhesion disc expressed as percentage [%]. α_{norm}: Mean normalized filling factor α_{norm} ± the standard deviation. In each case, the number of GUVs analyzed is given in brackets

Case	R_{adh} [%]	c_f^{max} [%]	α_{norm}
I	100 ± 1 (10)	2.5 (10)	1.00 ± 0.01 (5)
II	98 ± 1 (10)	2.0 (5)	0.96 ± 0.04 (4)
III	100 ± 1 (8)	1.5 (8)	0.98 ± 0.01 (5)
IV	86 ± 5 (5)	0.7 (5)	0.81 ± 0.05 (5)
V	92 ± 5 (16)	0.5 (41)	0.79 ± 0.07 (5)
VI	91 ± 5 (7)	0.5 (5)	0.90 ± 0.01 (6)

initially floppy, continued to be flaccid after adhesion as evidenced by fluctuating excess area. In some cases, at the center the inter-membrane distance was very high–30 nm or more–showing clearly that this region was not bound. In others, even though the distance at the center was not so high, about 10% of the vesicle membrane was nevertheless fluctuating.[27] The non-fluctuating adhered region formed an annular ring. Two distinct regions could be distinguished within the adhered region–a peripheral ring with inter-membrane distance of 5 nm and an inner region with inter-membrane distances of up to 15–20 nm.

Even at long times (up to three hours after addition of vesicles to the SLB sample) the adhesion did not proceed to completion. Interestingly, dilution of ligands on the GUV still led to complete adhesion as long as sufficient amounts of receptors were available (case II). At low receptor concentrations, the specific adhesion energy density achieved by bond formation was not high enough to deform or further spread the vesicle membrane. The global shape of the vesicle remained the same as it was in the gravity dominated weak unspecific adhesion state. This suggests that the contribution to the spreading pressure arising from the formation of bonds was small compared to the weak unspecific contribution.

Receptor distributions in the adhesion zone observed by fluorescence microscopy

Adhesion of the vesicle membrane to the SLB induced the accumulation of receptors in the adhesion zone which implies that initially free receptors outside the adhesion zone diffused into the zone and became bound. Such an accumulation can be expected from the thermodynamics of a system where both the receptors in the bilayer and the ligands in the GUV are mobile.[4] The extent and the pattern of the accumulation varied systematically with the initial composition of the SLB.

At initial receptor concentrations of 0.5% or higher (case I, II and III) receptors were accumulated homogeneously in the adhesion zone (see Fig. 2a and b). The maximum concentration reached within the adhesion zone c_f^{max} was mainly set by the initial concentration of receptors on the SLB while a change in ligand concentration on the GUV had a lesser effect on c_f^{max} (see Table 2). For example, doubling the receptor concentration from 0.5% to 1% (at ligand concentration 0.5%) increased c_f^{max} by 65% (from 1.5 to 2.5), but increasing the ligand concentration by a factor of five from 0.1% to 0.5% (at receptor concentration 1%), led to a relative increment in c_f^{max} of only 25% (from 2 to 2.5).

At initial receptor concentrations lower than 0.5% (case IV, V and VI), the accumulation of receptors was inhomogeneous and the adhesion zone was only partially filled (see Fig. 2c and d). The receptors were kinetically trapped in a ring along the periphery of the contact zone whereas at the center, no change in receptor concentration could be detected[28] (Fig. 2d). The maximum value of accumulation was reached in the middle part of the ring–accumulation decreased towards both edges of the ring. In all the low concentration cases, the maximum concentration c_f^{max} was smaller than in the higher concentration cases discussed before. Moreover, the effect of receptor and ligand concentration on c_f^{max} was different: 2.5 fold augmentation of the receptor concentration led only to an increase of 40% in c_f^{max} (from 0.5% to 0.7%), while five fold augmentation of the ligand concentration had no measurable effect at all—c_f^{max} stayed at 0.5%. Fig. 3

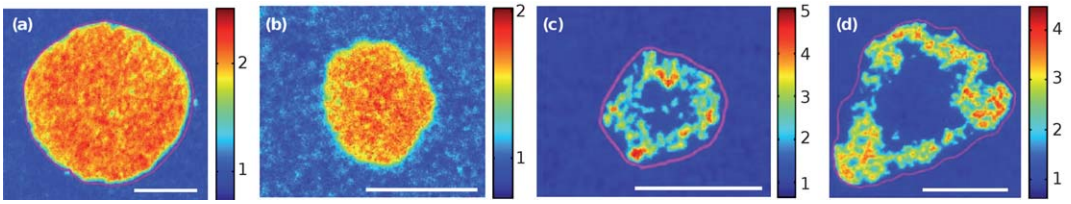

Fig. 2 Normalized fluorescence maps for representative vesicles in the final adhesion state. Cases presented are, from left to right, case I (1% SLB, 0.5% GUV), case II (1% SLB, 0.1% GUV), case V (0.1% SLB, 1% GUV), and case VI (0.1% SLB, 0.1% GUV). The color bar indicates the maximum accumulation index A^{max}. Scale bar: 10 μm.

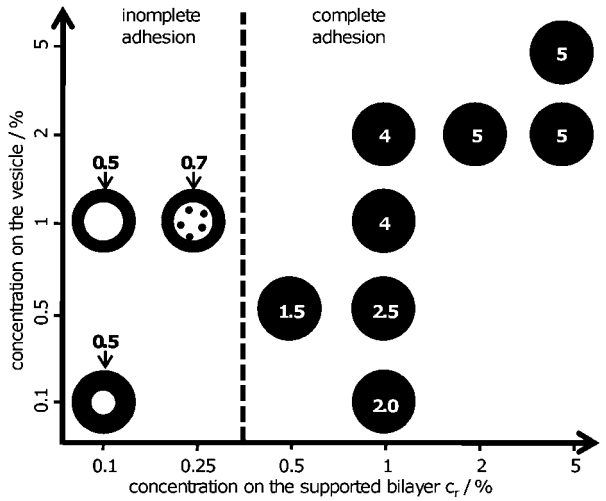

Fig. 3 Schematic representation of receptor accumulation (in black) at various initial concentrations of receptors on the supported bilayer and ligands on the vesicle. The maximum concentration reached in the contact zone c_r^{max} is marked for each case. Note that the geometrically possible maximal c_r^{max} of 5% is achieved only at high receptor concentrations. The dotted line separates the cases of complete and partial membrane adhesion.

summarizes the overall trends of receptor distribution and accumulation for different ligand–receptor concentrations.

The compactness or filling factor α_{norm}, which is a measure of the area covered by receptors within the adhesion zone, was calculated for five exemplary vesicles from each group. For cases I, II, III, corresponding to high receptor concentrations, α_{norm} was close to unity indicating full and compact filling. For cases IV, V, VI, corresponding to low receptor concentrations, α_{norm} was less than unity and indicated partial fractal-like filling (see Fig. 2). The fractal-like structure of the accumulated clusters is reminiscent of diffusion limited aggregates. Even though it is not possible to compare α_{norm} directly with a fractal dimension, the form of the clusters suggests that diffusion had contributed significantly to the formation process.

Impact of receptor concentration and diffusivity on bond accumulation

Since both receptors and ligands were bound to lipids in a fluid bilayer (the low phase transition temperature of SOPC ensured fluidity), their availability for participation in bond formation depended on their concentration as well as on diffusion. However, the two effects are not independent—diffusion of the receptors on the SLB is related to their concentration. With increasing concentration the receptors slow down till they immobilize completely when either closed packing of the receptors is reached or binding to ligands in a GUV takes place.[2] Therefore, in addition to a direct influence of concentration on the final adhesion state, an indirect influence *via* receptor diffusivity was expected. It should be noted that the receptors, with ~4 nm diameter were considerably larger than the ligands with ~0.5 nm diameter. Thus, receptors diffuse significantly slower than ligands, as confirmed by earlier measurements.[2] Therefore, the diffusion of the receptors rather than that of the ligands was expected to limit the effectiveness of filling.

Evidence that receptor diffusion is a sensitive parameter in determining receptor accumulation also came from complementary experiments at a higher temperature. At low temperatures (21 °C, as is the case for the experiments presented herein), a packing of maximum possible density, corresponding to 5%, was reached only if the initial receptor concentration was at least 2%. At the higher temperature of 37 °C on the other hand, this maximum was reached with a relatively low initial receptor concentration of 0.5%.[2] This provided additional evidence that the accumulation was strongly influenced by the temperature dependent diffusion constant of receptors.

The characteristic time scale of accumulation is set by the time a receptor needs to diffuse to its neighbor and form a cluster *via* binding to ligands in the GUV which in turn leads to immobilization. It is given by $\tau = x(c_r)^2/4D(c_r)$. τ Depends on the concentration c_r (expressed as the percentage of biotinylated lipids in the SLB) in two ways: on one hand, a higher initial c_r implies a reduction in the distance $x(c_r)$ between the receptor molecules, which facilitates accumulation; on the other hand, the receptor diffusivity $D(c_r)$ decreases with increasing c_r,[2] which could delay accumulation.

Assuming homogeneous distribution of receptors on the SLB, the average distance $x(c_r)$ between two neighboring receptors follows from geometrical considerations:

$$x(c_r) = 2\sqrt{\frac{a}{\pi c_r}} \tag{2}$$

with $a = A_{SOPC} = 0.7$ nm^2 being the area occupied by one SOPC lipid molecule. From theoretical considerations, an exponential decay of D with increasing concentration was expected:[29]

$$D(c_r) = D_0 \exp\left(-\frac{c_r}{c_r^*}\right) \tag{3}$$

Typical values of the parameters $D_0 = 0.45$ μm^2 s^{-1} and $c_r^* = 2\%$ were estimated from receptor diffusion data at receptor

concentrations of 1%, 2% and 5%. c_r^* is related to the critical concentration at which a displacement may occur. Finally, combining eqn (2) and 3, and using the definition of D resulted in a relation for $\tau(c_r)$:

$$\tau(c_r) = \frac{a}{\pi c_r D_0} \exp\left(\frac{c_r}{c_r^*}\right) \quad (4)$$

Fig. 4 illustrates the change of the characteristic time scale τ for bond accumulation with increasing receptor concentration for typical experimentally relevant parameters given above. As can be seen, at low receptor concentrations, the $1/c_r$ term dominated. As a result accumulation was expected to be inefficient. With increasing concentration the drop in tau slowed down due to the $\exp\left(\frac{c_r}{c_r^*}\right)$ contribution. This slowing down was moderate compared to the strong concentration dependence at low concentrations. Thus, the dominant effect of reducing c_r below about 0.5% was a rapid increase in characteristic accumulation time due to the scarcity of receptors.

It is important to understand why close packing of bonds could not be achieved at low concentrations even after a long waiting time. To answer this question, we need to consider the time over which a receptor can diffuse before its diffusion is halted or greatly reduced due to bond formation. At high concentrations of receptors, the time for a ligand to find a receptor is similar to the time for a receptor to diffuse up to its nearest neighbor (calculated to be about 0.2 msec for 0.1% ligands in the GUV and 1% receptors on the SLB). Thus, receptors had ample time to readjust their position to achieve the close packing state before they were bound and their mobility was reduced. At intermediate concentrations too, homogeneous filling was achieved by a similar mechanism even though the receptors did not have enough time to achieve close packing.

At the same ligand concentration, but at low concentrations of receptors, the typical time for ligand–receptor encounter is much smaller than the typical free diffusion time of the receptors themselves (about 10 times faster as calculated for 0.1% ligands in the GUV and 0.1% receptors on the SLB). At the same time,

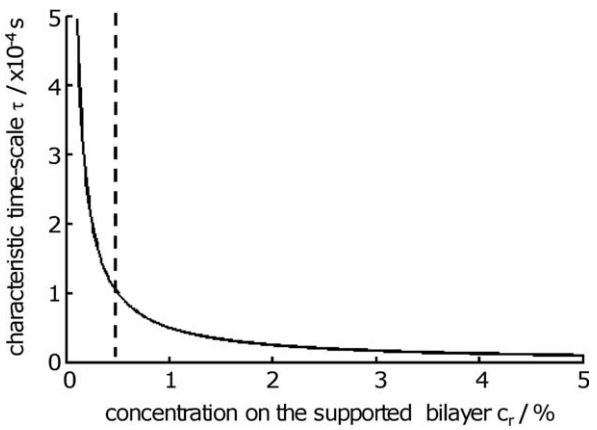

Fig. 4 The characteristic time scale of accumulation τ as a function of the initial receptor concentration c_r (see text for parameter values used, we verified that small changes in the values of the parameters does not change the result qualitatively). The dotted line separates the cases of complete and partial membrane adhesion.

the adhesion zone grows at ~2 μm^2 s^{-1} and overtakes the accumulation process, thus forestalling further filling of the adhesion zone. However, at the end of the spreading process, accumulation could still have proceeded up to full filling. This did not happen since now the receptors had to penetrate into an already formed adhesion zone. Before they could penetrate very far, they encountered ligands, were bound, and virtually immobilized. As more and more receptors accumulated, the environment got more and more crowded, leading to jamming of receptors into a glassy state.[2,30] When enough receptors were immobilized all along the edge of the adhesion zone, a continuous jammed annular cluster was formed and further filling was halted. In experiments where vesicles were re-examined seven hours after the initial adhesion, no evolution of the fluorescence map was detected, indicating that the annular cluster represents a very long lived or even steady state.

Origin of partial membrane adhesion

The question now arises whether the partial adhesion state of the membrane discussed before is a consequence of jamming. It turns out that while jamming is not directly responsible, it is indeed essential for achieving such a partially adhered state if ligands are abundant. Interestingly, in this state, the adhesion zone itself was inhomogeneous in terms of inter membrane distance h (see Fig. 1 II b). The height map reconstructed from the RICM movie revealed a ring of pronounced low h (5 nm) along the edge of the adhesion zone while the inter-membrane distance increased towards the center of the adhesion zone. In ref. 15 we showed that wherever receptors are accumulated, thus rising the local receptor concentration, the membrane is closer to the substrate due to formation of a dense array of bonds. Where receptors are not accumulated, the bonds are dilute and the average inter-membrane distance is higher. Note however, that the membrane in such dilute-bond clusters is still non-fluctuating and thus part of the adhesion zone. We could deduce the minimal concentration of receptors necessary to reach a completely adhered steady state to be 0.5%.

Receptor concentration and membrane binding. Partial membrane adhesion for strong binding pairs like biotin–neutravidin has not been reported so far.[7,8,31] The experimental conditions used in these studies (*i.e.* the receptor concentration employed) favored strong, complete adhesion. However, a hint about the origin of the partially bound state reported here comes from experiments with weak binding pairs like RGD–integrin ($E_a \sim 10\ k_BT$) or E-selectin–sialyl Lewis X ($E_a \sim 5\ k_BT$) where partial membrane binding has been described.[4,14,32,33] Indeed, it can be shown from thermodynamic arguments that for intrinsically strong bonds and a surplus of ligands, all the receptors should be bound leading to total binding of the membrane, whereas for weak bonds, at sufficiently low receptor concentrations, the membrane may be only partially bound. Here we present a proof of principle demonstration, under the assumption that there are excess ligands on the GUV and that receptors cannot penetrate into the adhesion zone. First note that since the size of the contact zone and hence the shape of the vesicle was not modified by adhesion at low receptor concentrations, the adhesion induced change in elastic energy was very small. Therefore, the main contribution to the change

in free energy ΔF came from the enthalpy due to bond formation and the change in entropy of the binding pairs. Following ref. 4, $\Delta F = E_a N_b + k_B T \ln \Omega$ where E_a is the enthalpy of bond formation of a single bond, N_b is the total number of bonds formed during adhesion and Ω represents the loss in the number of possible configurations of the system. Ω Consists of four terms accounting for the contribution of permuting (i) free receptors, (ii) free ligands, and (iii) bound receptors—all in the contact zone and, (iv) free ligands in the part of the vesicle membrane that does not form a part of the contact zone. For simplicity we make a few assumptions: (1) whenever a ligand is placed over a receptor, a bond is formed. The probability of bond formation is of course concentration dependant but here we take it to be unity. (2) The number of ligands and ligand sites on the GUV is very large compared to N_b, and there is no appreciable change in entropy of ligands after binding. Note, that the number of ligands is limited by the size of the GUV. Then, Ω has only terms (i) and (iii) and depends solely on the number of sites S_c available to the receptors, the concentration of receptors (written as the fraction c_r of S_c that was occupied by receptors) and the number of formed bonds (which could be written in terms of fraction q of receptors that are bound).

With these assumptions and using Stirling's formula:

$$\Omega = S_c c_r \ln(S_c c_r) - S_c c_r q \ln(S_c c_r q) - 2S_c c_r (1-q)\ln(S_c c_r (1-q)) - S_c(1 - c_r + c_r q)\ln(S_c(1 - c_r + c_r q))$$

for any given E_a and c_r, ΔF can now be calculated to determine the fraction q of the receptors that are going to be bound. Note here that in our system, due to the formation of the ring-like receptor cluster that isolates the interior of the adhesion zone from the exterior, the relevant part of the SLB is no longer connected to an infinite reservoir of receptors. Thus c_r gets fixed at its initial value and can not evolve.

At high E_a, no matter how low c_r was, the enthalpy term dominated and the energy was minimized by forming the maximum number of bonds possible. Thus, the minimum energy configuration was characterized by $q = 1$ (see Fig. 5a–c). At low E_a, on the other hand, the entropy term may successfully compete with the enthalpy term. At experimentally relevant $c_r = 0.25\%$, to get a q of 90% (corresponding to a 90% bound contact zone as observed in the experiment, see Fig. 1 and Table 2), E_a must be as low as 10 $k_B T$ (see Fig. 5d–f). It is worth noting here that the minimum q is very sensitive to E_a: at $E_a = 12\ k_B T$ it already shifts to 95% and at $E_a = 15\ k_B T$, the energy is again minimized for $q \sim 1$.

The contribution to the free energy coming from membrane fluctuations can be expected to depend on the membrane tension and is ignored in this calculation. Estimating this contribution following Seifert[34] shows that in the typical tension range expected for a GUV (10^{-7} to 10^{-5} N m^{-1}), the difference in F between the partially unbound low concentration case and the fully bound high concentration case is in fact very weakly dependent on tension. Assuming that in the former case, 10% of the area of unbound membrane resides at 20 nm and the bound membrane resides at 5 nm in both cases (as seen in Fig. S1, ESI†), the free energy density, at $\sim 10^{-8}$ J m^{-2}, is two orders of magnitude lower than in the case of weak adhesion. Thus ignoring contributions from membrane fluctuations is justified.

From the ideas presented above, in order to rationalize our observation of incomplete adhesion, we have to conclude that the binding energy of the biotin/neutravidin system employed here was much lower than the binding energy of 35 $k_B T$[35] measured in solution.

Competitive unbinding. To support our hypothesis of a relatively low effective binding energy in our system, we performed competitive unbinding experiments. Completely adhered GUVs (with ligand/receptor concentrations of 0.1% and 1% respectively) were exposed to free biotin molecules present in large excess in the external buffer which acted as antagonists to the biotin on the GUVs. After one hour of incubation, the sample was scanned in RICM mode and 10 exemplary GUVs were recorded. The area of the adhesion zone (normalized with respect to the area of the contact zone) reduced from 100% to 90–95%. The GUVs exhibited small bubbles in their former adhesion zone (Fig. 6 II b) and/or showed fluctuating edges. Fig. 6 shows the distribution of the measured heights in the contact zone of an exemplary GUV before (Fig. 6 I c) and one hour after (Fig. 6 II c) addition of free biotin. In this case, the peak of the distribution shifts from 8 nm to 11 nm. A further sign for unbinding is that the width of the height distribution also increases. Likewise more pixels with an increased fluctuation amplitude were detected in the fluctuation maps (Fig. 6 I d and II d). A control experiment in which only neat buffer was exchanged ruled out pure hydrodynamic effects as the source of the observed partial unbinding. Thus the de-adhesion of the membrane could be attributed to unbinding of some of the biotin-neutravidin bonds that initially held the GUV and SLB membranes firmly together.

Inter-membrane adhesion mediated by specific ligand/receptor bonds is stable against a very large range of concentrations of competitive binders in solution. In fact, the equilibrium number of inter-membrane bonds is a decreasing sigmoid function of the concentration of the competitor, where most changes occur within two orders of magnitude in the concentration of the soluble competitor. This reasonably fast drop is followed by an exponential-like decay (the tail of the sigmoid function) over several orders of magnitude in competitor concentration (see ref. 33 for details on the mechanisms for competitive inhibition of vesicle adhesion). From the concentration of soluble biotin used as the competitor in the current experiments, we can estimate that the binding affinity of biotins embedded in the membranes is considerably smaller than that of soluble biotin. Such antagonist induced de-adhesion of specifically adhered vesicles has been reported earlier in a model system where binding was mediated by weak, immobilized binding partners.[33]

Origin of low ligand–receptor binding energy. The lowering of the effective binding energy may have two origins: (i) biotinylated lipids were employed instead of isolated biotin molecules. The covalent binding of biotin molecules to the bulky head group of a lipid may have modified the effective binding chemistry of interaction of the biotin moiety with neutravidin.[36–38] (ii) The fact that the binders reside on a fluctuating two dimensional surface played a significant role.

To rule out the former possibility, unbinding of fluorescent neutravidin from the SLB in the absence of any GUV but in the presence of competing free biotin in solution was checked. In

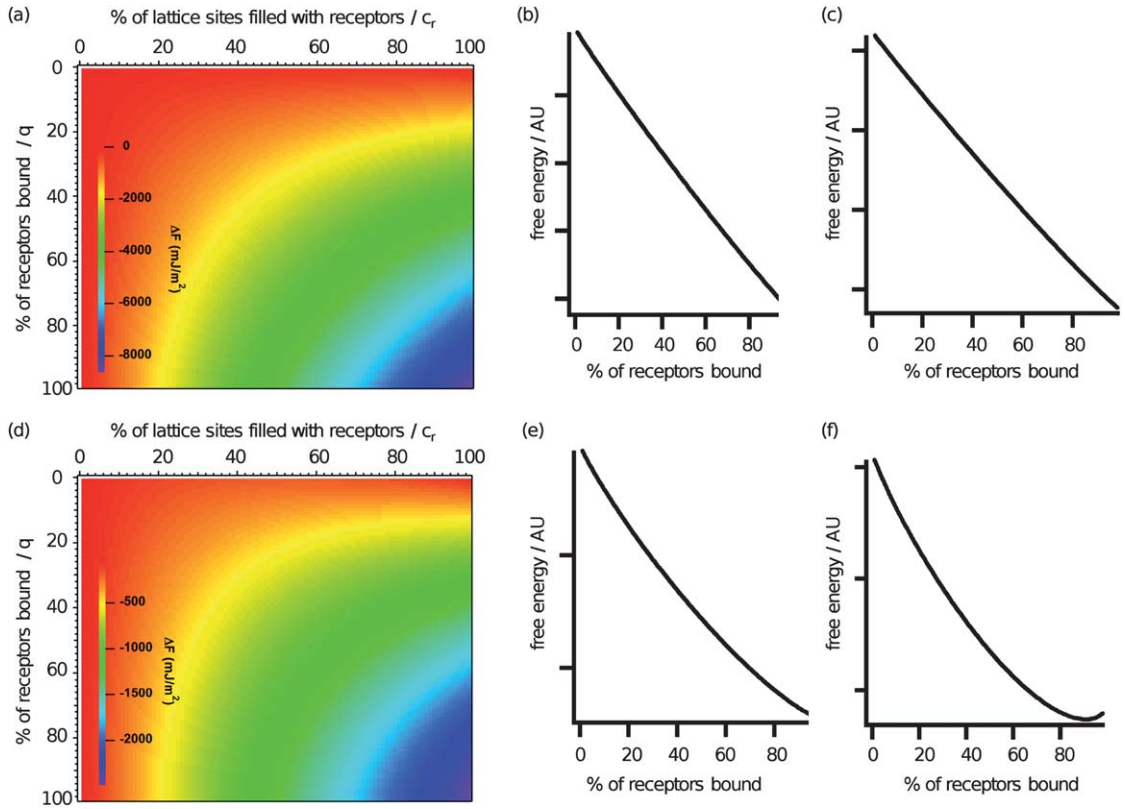

Fig. 5 Change in free energy ΔF resulting from binding of receptors in the adhesion zone, where a fraction c_r % of all the sites are occupied and of those, q % participate in bond formation. (a): ΔF As a function of c_r and q with affinity $E_a = 35\ k_BT$, (b): a cut through (a) at high receptor concentration ($c_r =$ 90%), (c): a cut through (a) at low receptor concentration ($c_r = 0.25\%$), (d): same as (a) with $E_a = 10\ k_BT$ (e): a cut through (d) at high receptor concentration ($c_r = 90\%$), (f): a cut through (d) at low receptor concentration ($c_r = 0.25\%$).

these control experiments, no unbinding was detected for incubation periods of up to 90 min indicating that within the time scale of our experiments on antagonist induced unbinding of GUVs, the ligand/receptor bond by itself was stable against competitive unbinding. In order to minimize bleaching effects the sample was imaged only every 30 min. The spatial and temporal variation of the detected intensity in these images was of the order of 3%. Thus, a 10% decrease could be ruled out. This observation argues against the hypothesis that the chemical modification of the biotin moiety played a significant role. We can therefore attribute the lowering of the effective binding affinity to the effect of confining the reacting pair to two difference fluctuating surfaces.

That the biotin/neutravidin system, with an expected intrinsic binding energy of about 35 k_BT, in fact exhibited a much lower effective energy could be understood in the light of a recently proposed theory linking receptor concentration and effective binding affinity (or bond strength)[14] if the receptors are bound to

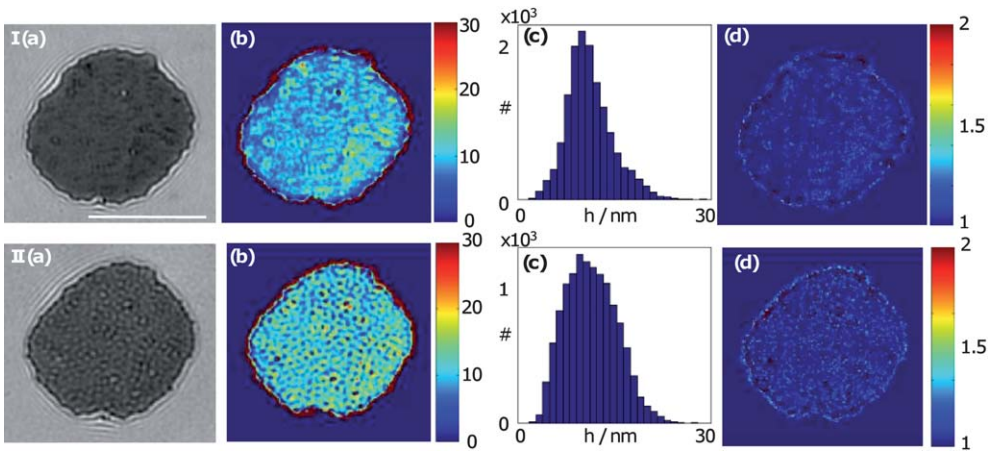

Fig. 6 Exemplary vesicle before (I) and one hour after (II) addition of free biotin. (a) Mean RICM image. (b) Height map [nm]. (c) Histogram showing the height distribution. (d) Normalized fluctuation map. Scale bar 10 μm.

a flexible membrane. Initially, when the membrane in the contact zone exhibits strong fluctuations as reported above, it resides in a shallow secondary minimum of the membrane/substrate interaction potential. After specific adhesion, the membrane goes to the deep global minimum of the interaction potential due to the formation of bonds. If the membrane is bound by a dense cluster of bonds, cooperative effects stabilize the bonds.[13] However, if it is bound with only a sparse distribution of bonds—as in the present case at low receptor concentrations, the parts of the membrane that are not pinned by bonds have a tendency to fluctuate and access the secondary minimum, thus exerting a force on the bonds and weakening them.[14]

4 Conclusion

We have shown that when membrane adhesion is mediated by sparsely distributed but mobile and bulky linkers, a stable annular adhesive junction forms spontaneously (Fig. 3). This is in contrast to the much studied strong adhesion case[7,8,31] where the inter-membrane interface is homogeneous both in terms of inter-membrane distance and ligand–receptor distribution. Scarcity of receptors leads to inhomogeneity. In the present system, both the homogeneous and the inhomogeneous states are obtained as the concentration of receptors is varied (as summarized in Table 3).

Let us first consider the case of high receptor concentration. The receptors diffuse into the contact zone and fill it up as we reported earlier.[2] Since the bond enthalpy of the avidin/biotin linkers is rather high, the change in free energy due to formation of numerous bonds is dominated by the total enthalpic contribution—the system therefore maximizes the number of bonds, leading to two effects. The first is, that all the available excess-area of the flaccid vesicle is used for expanding the contact area between the vesicle and the supported membrane, resulting in deformation of the vesicle. The vesicle shape at the steady state is determined by a balance of elastic deformation, costing free-energy, and the spreading pressure that results from the formation of bonds.[4] The loss of excess area is responsible for the suppression of fluctuations in the entire vesicle due to the increasing tension. The second effect arises because the receptors are mobile and can diffuse into the spreading adhesion disc. Once inside they are quickly bound and become effectively immobile. This leads to further accumulation of receptors from the bulk of the substrate into the inter-membrane contact zone and then into the adhesion zone. While the accumulation itself arises purely because of thermodynamic reasons,[4] membrane deformation and/or fluctuation mediated correlations between bonds aid in their compaction and organization.[13–15] In the present case, though the receptors are bulky and hence slowly diffusing, when present in sufficient numbers (>2% of the lipids in the supported membrane are functionalized), they are able to fill the adhesion disc to the limit of geometrical close packing during the initial growth of the domain. At intermediate concentrations ($0.5\% \geq c_r < 2\%$ functionalized lipids), the filling is homogeneous but the limit of geometrical close packing is not reached. Nevertheless, in the final state, the receptors in the adhesion zone are jammed. Further increase of binder concentrations results in close packing. Very similar accumulation of receptors has been observed between adhering cells[39,40] and between cells adhered to bilayers.[11,16] In cells however, the concentration of binders is very low—typically about 10^2 per μm^2. In our model system, we were able to systematically vary the binder concentrations and go down to concentrations close to those relevant in cells.

At low concentrations of receptors (≤0.5% of the lipids are functionalized), if the enthalpy of the ligand–receptor bonds is not too high, the change in free energy due to bond formation is no longer dominated by the enthalpic contribution of bond formation, but the loss of entropy associated with bond formation is equally important.[10] Therefore the system no longer necessarily maximizes the number of bonds, but a fraction of free binders is available. This introduces several important differences with respect to the case discussed above. First, the formation of bonds is not sufficient to build up a spreading pressure that could change the overall shape of the vesicle. Therefore, the inter-membrane contact zone does not change due to adhesion. The initially flaccid vesicle remains floppy and the fluctuations are suppressed only within regions where the membrane is pinned down by an array of bonds. Second, even if the ligands and receptors are free to diffuse, the minimum energy configuration does not necessarily correspond to the one where the contact zone is filled with bonds. When the enthalpy associated with a single bond is very low, for example for

Table 3 Schematic representation of the important differences between the cases of (a) high ($c_r \geq 0.5\%$) and (b) low ($c_r < 0.5\%$) initial receptor concentration.

	(a)	(b)
	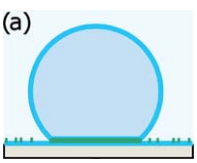	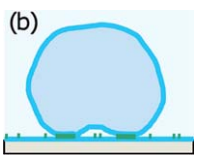
Initial receptor concentration on the supporting membrane (SLB)	≥0.5%	<0.5%
Initial ligand concentration in the membrane of the vesicle (GUV)	independent	independent
equilibrium determined by balance of:	bond ↔ membrane deformation	bond enthalpy ↔ bond entropy
membrane adhesion	complete	incomplete
bond distribution	homogeneous	ring-like
maximum receptor concentration in the adhesion zone	$1\% < c_r < 5\%$	$c_r < 0.7\%$
membrane tension after adhesion	high	low
inter-membrane distance	homogeneous 5–10 nm	inhomogeneous 5–50 nm

integrin/RGD interaction, small patches of adhesion domains are formed.[4] In the current case the bond enthalpy is somewhat larger than in the integrin case which imposes, according to our calculations, that the adhesion zone should be eventually filled with receptors, no matter how low the initial concentrations. These calculations are based on the thermodynamic arguments (see ref. 4 for details) and assume that the mobile unbound receptors are coupled to a reservoir of constant receptor concentration provided by the bulk of the supported membrane.

In the present case however, full filling does not happen because the slowly diffusing sparsely distributed receptors are not able to fill the adhesion domain as it grows. After the contact zone is established, receptors continue to diffuse into the newly formed adhesion zone. They however are able to diffuse only a short distance before they are bound and immobilized. Thus, a region of high receptor density builds up along the periphery. Eventually, a closed continuous annular cluster of immobilized and jammed receptors is formed. The fractal like ultrastructure of this closed cluster points to a diffusion limited growth process. We find that the final density achieved in this dense cluster depends on the initial concentrations—the receptors are not necessarily closely packed to the geometrically allowed limit. However, the jammed peripheral ring effectively seals off the interior against further exchange of receptors with the outside. Thus, the receptor concentration at the center of the contact zone remains at the initial low level.

The inter-membrane distance in the region of contact reflects the underlying receptor clustering. At the peripheral ring, where the receptors are accumulated to a high density, the inter-membrane distance is low—that is to say that the membranes are tightly bound, just like in the high concentration case. In the region where the receptor accumulation is low or undetectable, the inter-membrane distance is variable. At the very center the vesicle membrane is far from the supported membrane, and fluctuating, indicating that the central region is free of bonds. Often, surrounding the central bond-free region, but inside the outer annulus just described, there is another annular region where the membrane does not fluctuate. The inter-membrane distance is slightly higher than in the peripheral ring but considerably less than in the central part where there are no bonds. Nevertheless, fluorescence data does not show any significant accumulation of receptors. This kind of adhesion domain corresponds to a dilute distribution of bonds.[15] Overall, about 10% of the membrane in the contact zone continues to fluctuate - assuming a homogeneous initial receptor distribution, about 90% of the receptors that were initially present are finally bound.

The jamming of receptors in the contact zone prevents the achievement of a thermodynamic lowest energy state with respect to receptor distribution (homogeneous close packing). However, it leads to a steady state in which the formation of ligand–receptor bonds is expected to proceed to thermodynamic equilibrium within the constraints imposed by the distribution of mostly immobilized receptors. This is supported by the clear separation of time scales regulating receptor diffusion and ligand–receptor reaction rate. We have presented thermodynamic arguments which show that the effective affinity of the avidin–biotin bond must be much lower than the high values previously measured in solution.[35] This conclusion is further strengthened by de-adhesion experiments in which soluble ligand was used as a competitor for the adhesion sites. Partial de-adhesion is observed and indicates that successful competition takes place at experimentally accessible time-scales, suggesting that the life-time of the biotin–neutravidin bond and the binding strength is smaller than expected.

One may ask why at such low bond strengths, there is no reorganization of the annular cluster due to bond kinetics, thus un-jamming the system and permitting it to proceed to a stable equilibrium represented by the fully filled state. The answer probably lies in the fact that there is a relatively strong excluded volume interaction among the bulky neutravidin molecules, as hinted at by the formation of a glassy state at high receptor concentrations,[2,30] which prevents disassembly of the cluster even though binding and unbinding processes permanently occur.

The observed structured steady state is made possible by an interplay of ligand/receptor concentration, their in-plane diffusivity and their effective binding energy—physical quantities that are expected to be also important in inter-cell adhesion. It is of course known that cells control adhesion through expression of receptors/ligands on their surface. The present results suggest that in addition to employing different receptor/ligand pairs, cells may be able to regulate the effective binding affinity of individual bonds by careful control of the surface concentration and spatial arrangement of the receptors. Strikingly, the bull's-eye pattern of receptors in the present system is strongly reminiscent of the characteristic shape of the immunological synapse, the physics of whose assembly is still being debated in the literature.[41]

5 Experimental

Materials

All lipids, SOPC (1-stearoyl-2-oleoyl-sn-glycero-3-phosphocholine), DOPE-PEG2000 (1,2-dioleoyl-sn-glycero-3-phosphoethanolamine-*N*-(methoxy(polyethyleneglycol)-2000)) and DOPE-cap-biotin (1,2-dioleoyl-sn-glycero-3-phosphoethanolamine-*N*-(cap biotinyl)) were from Avanti Polar Lipids (Alabaster, AL). Neutravidin covalently linked to the fluorescent label Oregon Green or tetramethylrhodamine (neutravidin-fl, both Invitrogen, Eugene, OR), as well as bovine serum albumin (BSA, 98% purity, Sigma, Saint Louis, MO) were reconstituted in PBS buffer and ultracentrifugated to eliminate protein aggregates.

Sample preparation

SLBs were prepared with a film balance (Nima, Coventry, UK) applying the Langmuir–Blodgett (proximal layer, pure SOPC) and Langmuir–Schäfer (distal layer, SOPC with 2 mol% DOPE-PEG 2000; 0.1, 0.25, 0.5 or 1 mol% DOPE-cap-Biotin) techniques. After preparation SLBs were passivated with BSA, incubated with neutravidin-fl in large excess, and again passivated by 15 min incubation in 0.5% BSA solution. After each binding step, excess protein was removed by exchanging the buffer against protein free PBS in a series of typically ten washing steps. GUVs consisting of SOPC with 2 mol% DOPE-PEG2000 and 0.1, 0.5 or 1 mol% DOPE-cap-Biotin were produced *via* electro-swelling as described before.[2] The osmotic difference between the swelling buffer (230 mOsm/l sucrose) and the measuring buffer (300 mOsm/l PBS) ensured that the vesicles

exhibited considerable excess area. Osmolarites and refractive indices of the solutions were measured with an osmometer (Osmomat 030, Gonotec GmbH, Berlin, Germany) and an Abbé refractometer (AR4D, Krüss, Hamburg, Germany), respectively. The prepared GUVs had diameters of about 20–30 μm.

Adhesion and de-adhesion experiments

In a typical adhesion experiment, 10 μL of the vesicle solution was added to the functionalized SLB in a total volume of 1 mL. Vesicles were allowed to sediment and achieved a steady adhesion state before the first measurement. The waiting time depended on the receptor and ligand concentrations. The specificity of binding of neutravidin to the biotinylated SLB, as well as that of the biotinylated GUV to the neutravidin coated SLB was verified. In the competitive un-binding or de-adhesion experiments, completely adhered vesicles were exposed to free biotin in solution by carefully removing 400 μl of the outer buffer (total volume 1 mL) and replacing it by an equal amount of iso-osmolar buffer containing 0.2 mg ml^{-1} biotin. All experiments were carried out at 21 °C unless otherwise stated.

Image acquisition

All images were acquired with an inverted microscope (Axiovert200, Carl Zeiss, Göttingen, Germany) equipped with a digital CCD camera (sensicam qe, PCO, Kehlheim, Germany) and a metal halogenide lamp (X-Cite, Exfo, Quebec, Canada). Image sequences were recorded in reflection interference contrast microscopy (RICM), fluorescence microscopy and phase contrast microscopy using a 63 × Antiflex Plan-Neofluar 1.25 oil objective with a numerical aperture of 1.25 and a built in lambda quarter plate. For RICM, the green illumination was selected using an interference filter (546 ± 12 nm) and crossed polarizers were introduced in the filter-cube to take advantage of the antiflex technique. The numerical aperture of illumination was set to approximately 0.5. Image sequences consisted of 50 consecutive frames with an individual exposure time of 100 ms. For fluorescence microscopy, the filter set appropriate for Oregon Green or tetramethylrhodamine was used. Fluorescence snapshots were recorded with illumination times of 100 ms with a fully open illumination aperture.

Acknowledgements

A.-S. S. acknowledges funding by the Deutsche Forschungsgemeinschaft DFG-SE 1119/2-1 and the Grant 22/08 of the Unity through Knowledge Fund, Croatia.

Notes and references

1 A.-S. Smith and E. Sackmann, *ChemPhysChem*, 2009, **10**, 66–78.
2 S. Fenz, R. Merkel and K. Sengupta, *Langmuir*, 2009, **25**, 1074–1085.
3 K. Sengupta and L. Limozin, *Phys. Rev. Lett.*, 2010, **104**, 088101.
4 A.-S. Smith, K. Sengupta, S. Goennenwein, U. Seifert and E. Sackmann, *Proc. Natl. Acad. Sci. U. S. A.*, 2008, **105**, 6906–6911.
5 Y. Li, R. Lipowsky and R. Dimova, *J. Am. Chem. Soc.*, 2008, **130**, 12252–3.
6 T. Gruhn, T. Franke, R. Dimova and R. Lipowsky, *Langmuir*, 2007, **23**, 5432–5439.
7 D. Cuvelier and P. Nassoy, *Phys. Rev. Lett.*, 2004, **93**, 228101.
8 P.-H. Puech, V. Askovic, P.-G. de Gennes and F. Brochard-Wyart, *Biophys. Rev. Lett.*, 2006, **1**, 85–95.
9 E. Sackmann and R. F. Bruinsma, *ChemPhysChem*, 2002, **3**, 262–269.
10 A.-S. Smith and U. Seifert, *Soft Matter*, 2007, **3**, 275–289.
11 M. L. Dustin, *J. Biol. Chem.*, 1997, **272**, 15782–15788.
12 M. Nguyen-Duong, K.-W. Koch and R. Merkel, *Europhys. Lett.*, 2003, **61**, 845–851.
13 H. Krobath, B. Rozycki, R. Lipowsky and T. R. Weikl, *Soft Matter*, 2009, **5**, 3354–3361.
14 E. Reister-Gottfried, K. Sengupta, B. Lorz, E. Sackmann, U. Seifert and A.-S. Smith, *Phys. Rev. Lett.*, 2008, **101**, 208103.
15 A.-S. Smith, S. Fenz and K. Sengupta, *Europhys. Lett.*, 2010, **89**, 28003.
16 M. A. McClosenky and M. M. Poo, *J. Cell Biol.*, 1986, **102**, 2185–96.
17 A. Tozeren, K. L. P. Sung and S. Chien, *Biophys. J.*, 1989, **55**, 479–487.
18 D.-M. Zhu, M. L. Dustin, C. W. Cairo and D. E. Golan, *Biophys. J.*, 2007, **92**, 1022–1034.
19 T. A. Ryan, J. Myers, D. Holowka, B. Baird and W. W. Webb, *Science*, 1988, **239**, 61–64.
20 J. J. Sieber, K. I. Willig, C. Kutzner, C. Gerding-Reimers, B. Harke, G. Donnert, B. Rammer, C. Eggeling, S. W. Hell, H. Grubmueller and T. Lang, *Science*, 2007, **317**, 1072–1076.
21 L. Limozin and K. Sengupta, *ChemPhysChem*, 2009, **10**, 2752–2768.
22 L. Limozin and K. Sengupta, *Biophys. J.*, 2007, **93**, 3300–3313.
23 C. Monzel, S. F. Fenz, R. Merkel and K. Sengupta, *ChemPhysChem*, 2009, **10**, 2828–2838.
24 Camera read-out noise and dark current were negligible.
25 The box counting algorithm uses parts of the box count function written by F. Moisy (University Paris-Sud) available through the MathWorks user community file exchange. http://www.mathworks.com/matlabcentral/fileexchange/.
26 U. Seifert and R. Lipowsky, *Phys. Rev. A: At., Mol., Opt. Phys.*, 1990, **42**, 4768–4771.
27 The fluctuating area occurs at the center and/or at the very edge of the adhesion zone where the vesicle membrane starts curving away from the supported bilayer.
28 A partial exception was case IV, where, in addition to the ring, numerous small accumulation clusters were observed well within the adhesion disc.
29 M. H. Cohen and D. Turnbull, *J. Chem. Phys.*, 1959, **31**, 1164–1169.
30 M. R. Horton, C. Reich, A. P. Gast, J. O. Rädler and B. Nickel, *Langmuir*, 2007, **23**, 6263–6269.
31 J. Fattaccioli, J. Baudry, N. Henry, F. Brochard-Wyart and J. Bibette, *Soft Matter*, 2008, **4**, 2434–2440.
32 Z. Guttenberg, A. R. Bausch, B. Hu, R. Bruinsma, L. Moroder and E. Sackmann, *Langmuir*, 2000, **16**, 8984–8993.
33 A.-S. Smith, B. G. Lorz, U. Seifert and E. Sackmann, *Biophys. J.*, 2006, **90**, 1064–1080.
34 U. Seifert, *Phys. Rev. Lett.*, 1995, **74**, 5060–5063.
35 C. A. Helm, W. Knoll and J. N. Israelachvili, *Proc. Natl. Acad. Sci. U. S. A.*, 1991, **88**, 8169–8173.
36 N. M. Green, in *Methods in Enzymology*, ed. M. Wilchek and E. A. Bayer, Academic Press, London, 1990, 184, 51–67.
37 K. Fujita and J. Silve, *Biotechniques*, 1993, **14**, 608–617.
38 J. DeChancie and K. N. Houk, *J. Am. Chem. Soc.*, 2007, **127**, 5419–5429.
39 C. Ocklind, U. Forsum and B. Obrink, *J. Cell Biol.*, 1983, **96**, 1168–1171.
40 M. Schmelz, R. Duden, P. Cowin and W. W. Franke, *Eur. J. Cell Biol.*, 1986, **42**, 184–199.
41 T. R. Weikl, J. T. Groves and R. Lipowsky, *Europhys. Lett.*, 2002, **59**, 916–922.

